SPECTRAL SIGNATURES FROM EVOLVING BLACK HOLE ACCRETION RINGS

Vladimír Karas[1)] & Marcel Štolc[1,2)]

1) Astronomical Institute, Czech Academy of Sciences, Prague

2) Faculty of Mathematics and Physics, Charles University, Prague

AXRO Meeting, Prague 2022

Nature Vol. 254 March 27 1975

5 Hooke, R., *Micrographia* (London, 1665).
6 *The Diary of Robert Hooke* 1672–1680 (edit by Robinson, H. W., and Adams, W.) (Taylor and Francis, London, 1953).
7 Birch, Th., *The History of the Royal Society of London*, 3 (London, 1757).
8 Mach, E., *Die Prinzipien der physikalischen Optik* (Barth, Leipzig, 1921); *The Principles of Physical Optics* (Dover, New York).
9 Gunther, R. T., *Early Science in Oxford*, **8** (printed for the author, Oxford, 1931).
10 Hannes, H., *Optik*, **13**, 34–48 (1956).
11 Huygens,
12 Huygens,
13 Huygens,
14 Riekher,
15 Smith, R.,
16 Thomin,
17 *Cours co*
{Pezena

articles

Possible power source of Seyfert galaxies and QSOs

J. G. Hills

Department of Astronomy, University of Michigan, Ann Arbor, Michigan 48104

The possible presence of massive black holes in the nuclei of galaxies has been suggested many times. In addition, there is considerable observational evidence for high stellar densities in these nuclei. I show that the tidal breakup of stars passing within the Roche limit of a black hole initiates a chain of events that may explain many of the observed principal characteristics of QSOs and the nuclei of Seyfert galaxies.

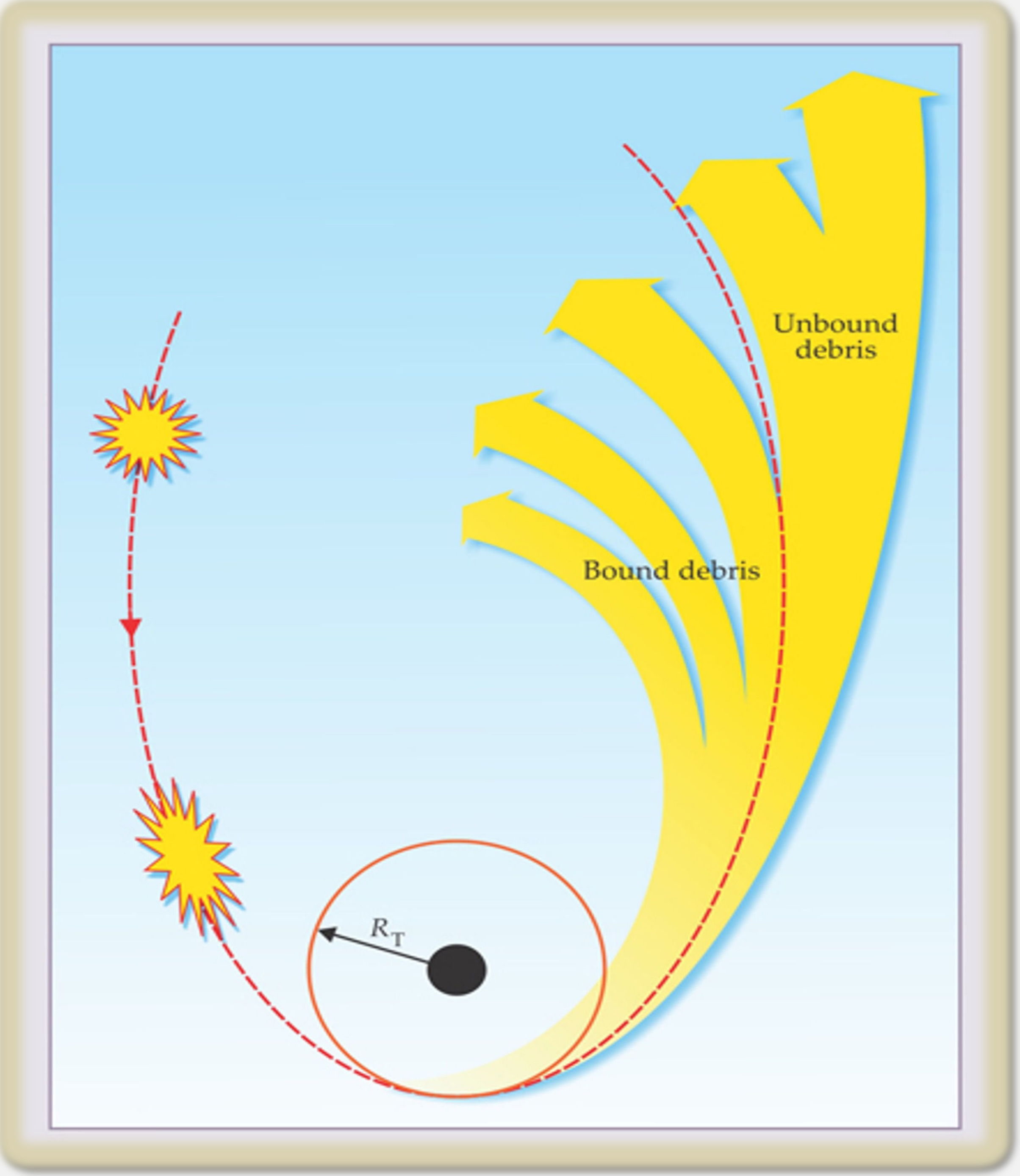

Tidal disruption of stars by black holes of 10^6–10^8 solar masses in nearby galaxies

Martin J. Rees

Institute of Astronomy, Madingley Road, Cambridge CB3 0HA, UK

Stars in galactic nuclei can be captured or tidally disrupted by a central black hole. Some debris would be ejected at high speed; the remainder would be swallowed by the hole, causing a bright flare lasting at most a few years. Such phenomena are compatible with the presence of 10^6–10^8 $M_\odot$ holes in the nuclei of many nearby galaxies. Stellar disruption may have interesting consequences in our own Galactic Centre if a $\sim 10^6$ $M_\odot$ hole lurks there.

$$r_T \simeq 5 \times 10^{12} M_6^{1/3} (r_*/r_\odot)(m_*/m_\odot)^{-1/3} \text{ cm}$$

M_6 denotes the hole's mass in units of 10^6 $M_\odot$. Esse

About half of the gaseous stellar debris remain gravitationally bound in highly eccentric elliptical orbits that bring it back over a course of months to years.

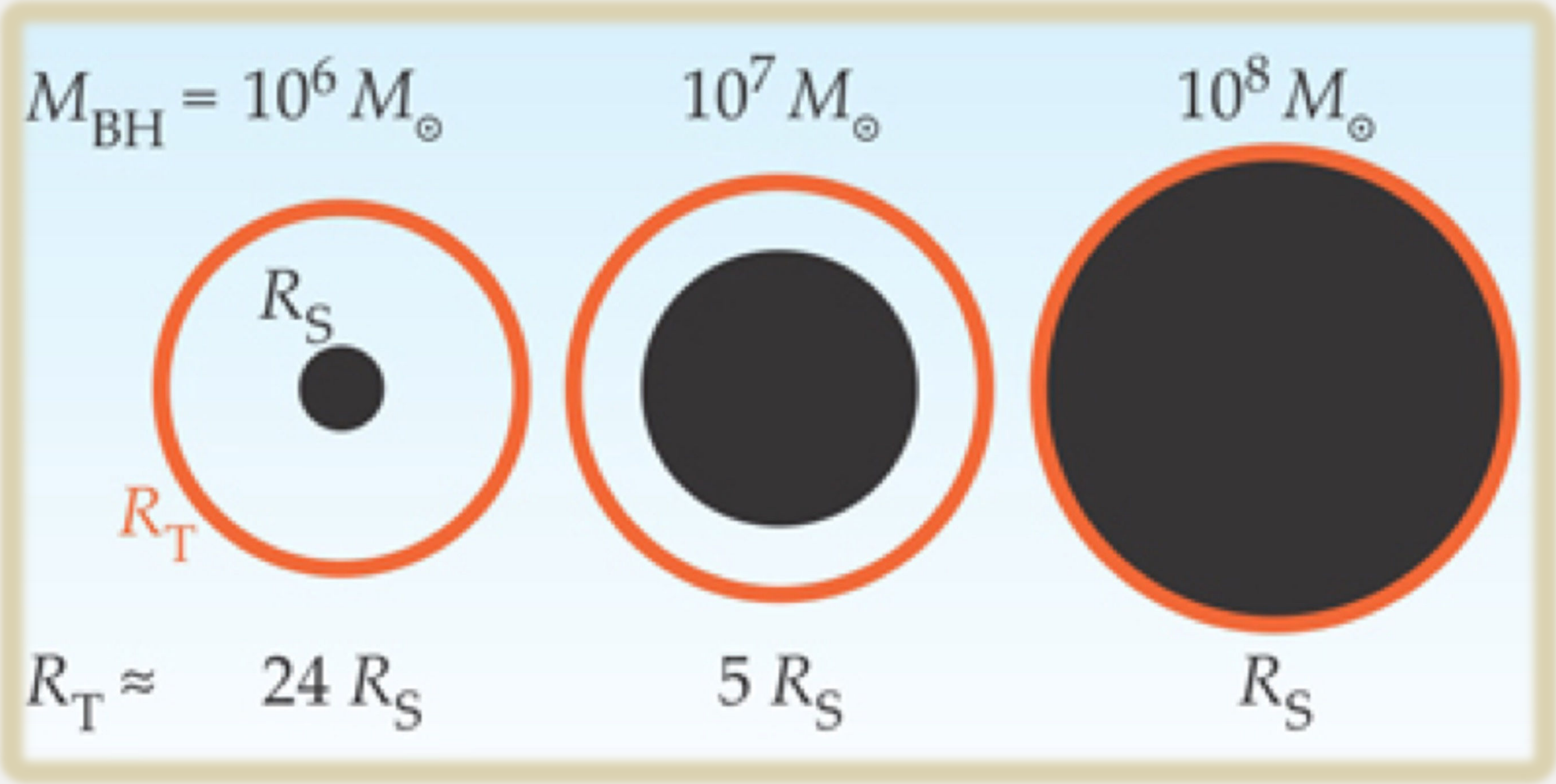

For Sun-like star, R_S and R_T become equal at $M_{BH} \approx 10^8\,M_\odot$.

TDE by a (non-spinning) black hole heavier than $10^8\,M_\odot$ cannot be seen.

(Gezari 2014)

XJ1500+0154

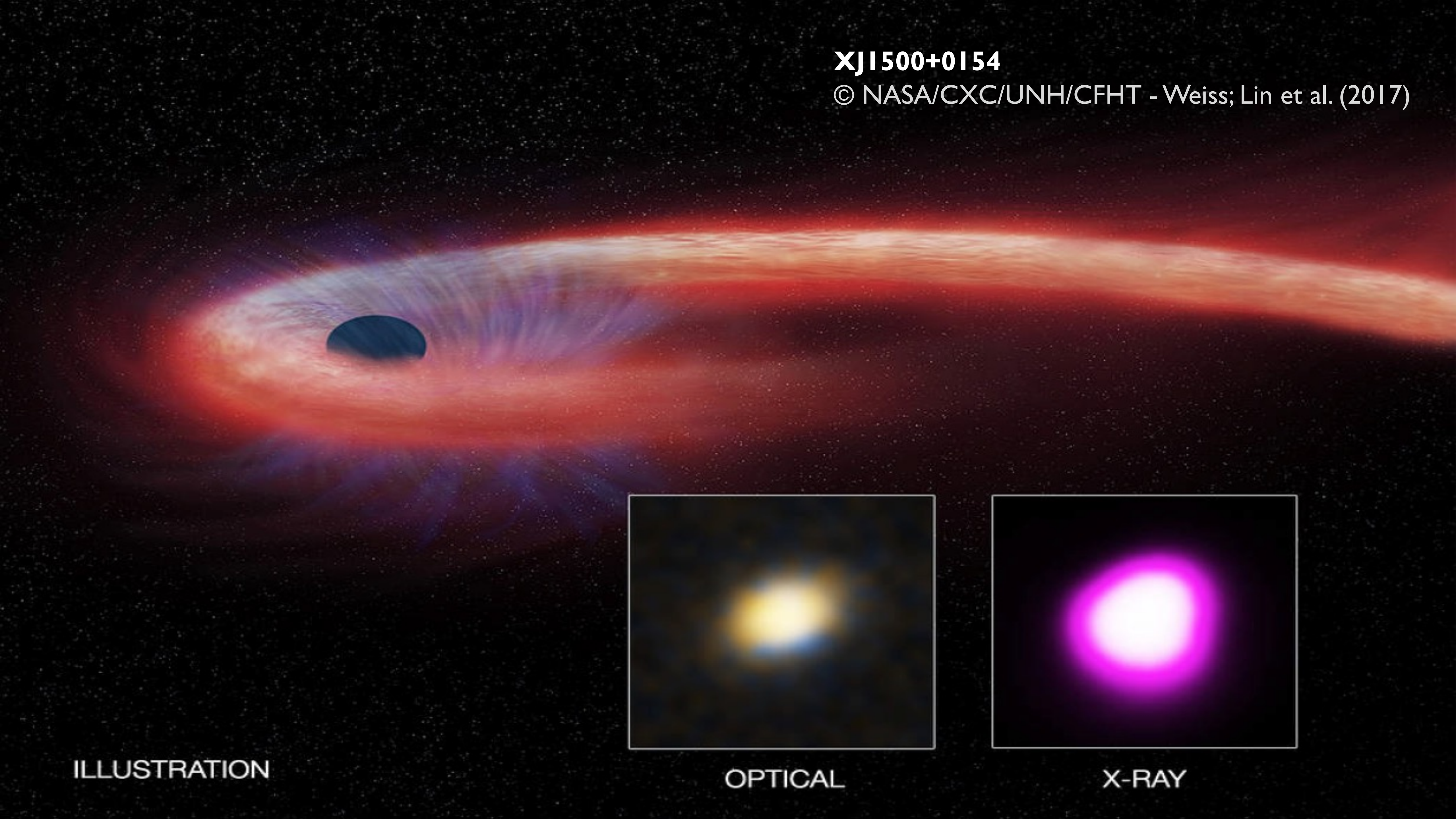

passing object (mass M_*, $\mathrm{radius}\,\mathrm{R}_*$) around a central body, e.g. neutron star or black hole (mass M_{BH}) gets ripped apart by the tidal forces due to central object's strong gravity after reaching tidal radius [Hills, 1975; Rees, 1985] defined as

$$\boxed{R_{\mathrm{tidal}} = \left(\frac{M_{\mathrm{BH}}}{M_*}\right)^{\frac{1}{3}} R_*}$$

TDE signposts:

- bolometric luminosity decline $t^{-\frac{5}{3}}$
- no activity (of the galactic nucleus) observed prior to the tidal disruption
- soft X-ray spectra hardening with passing time
- high intensity $10^{45} - 10^{46}\,\mathrm{erg.s}^{-1}$

Case of Changing Look AGN 1ES 1927+652

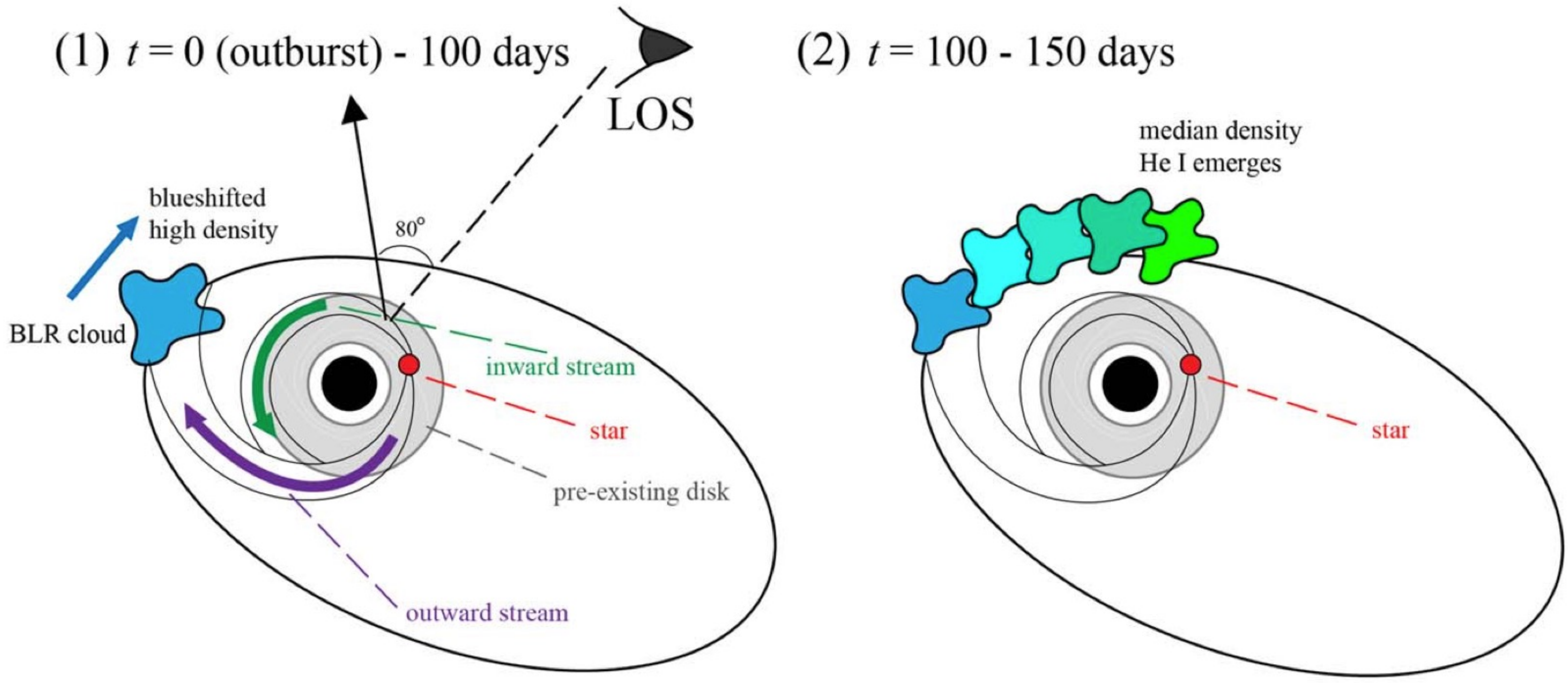

Ruancun Li, Luis Ho et al., (2022), ApJ

A very luminous jet from disruption of a star by a massive black hole

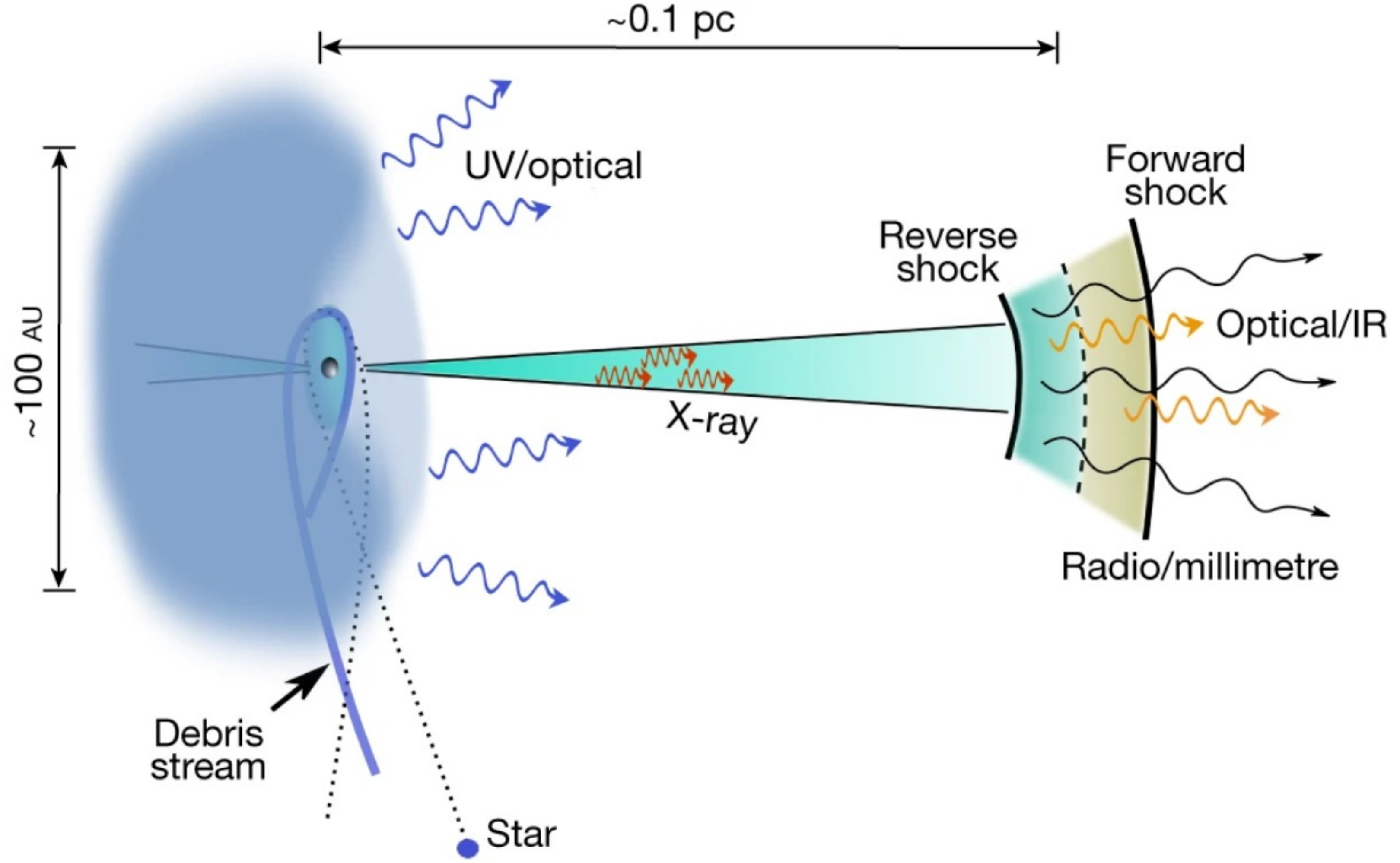

This illustration offers a visual representation (not to scale) of the physical processes explained in the text. Black dotted line: original geodesic of the star (note the general-relativistic apsidal precession). Thick blue line: the stellar debris gas undergoing self-intersection. Thick blue envelope of size approximately 100 AU (or 10^{15} cm; AU, astronomical units): optically thick gas (probably an outflow) reprocessing the X-rays and extreme-UV emission from the accretion disk into the UV/optical band, as observed from other non-jetted TDEs. Light blue disk of size approximately 1 AU (of the order of the tidal disruption radius): accretion disk near the black hole. Light blue cones: relativistic jets launched from the innermost regions of the disk. Shocks at a distance of approximately 0.1 pc (or 3×10^{17} cm) from the black hole: reverse shock dominates the radio/millimetre emission, and both reverse shock and forward shock contribute to the non-thermal optical/IR emission.

- Andreoni et al. (2022), Nature

1. $Q \ll 1$ ($r_g \ll r_t \ll R_\star$): A weak Newtonian tidal interaction, where the star's self-gravity and pressure dominate. Relevant when a stellar BH is swallowed by a star, and can result in an exotic star powered by accretion (e.g. Thorne & Zytkow 1975).
2. $Q \sim 1$ ($r_g \ll r_t \sim R_\star$): A strong Newtonian tidal interaction with significant mass loss and possible disruption, such as occurs in a close interaction between a stellar BH and a massive star (Sec. 4.3.2).
3. $Q \sim (c/v_\star)^2$ ($R_\star \sim r_g < r_t$): A complete disruption in the Newtonian regime, as would be the case for disruption by an IMBH.
4. $(c/v_\star)^2 < Q < (c/v_\star)^3$ ($R_\star \ll r_g < r_t$): A complete tidal disruption by a lower-mass MBH of the type considered here (e.g. Sgr A*), which can be treated as Newtonian to a good approximation[18].
5. $Q > (c/v_\star)^3$ ($R_\star \ll r_t \ll r_g$): Tidal disruption inside the event horizon. The star plunges into the MBH as a point particle on a GR trajectory.

TDE classification by $Q = (R_T/R_*)^{1/3}$ *(Alexander 2017)*

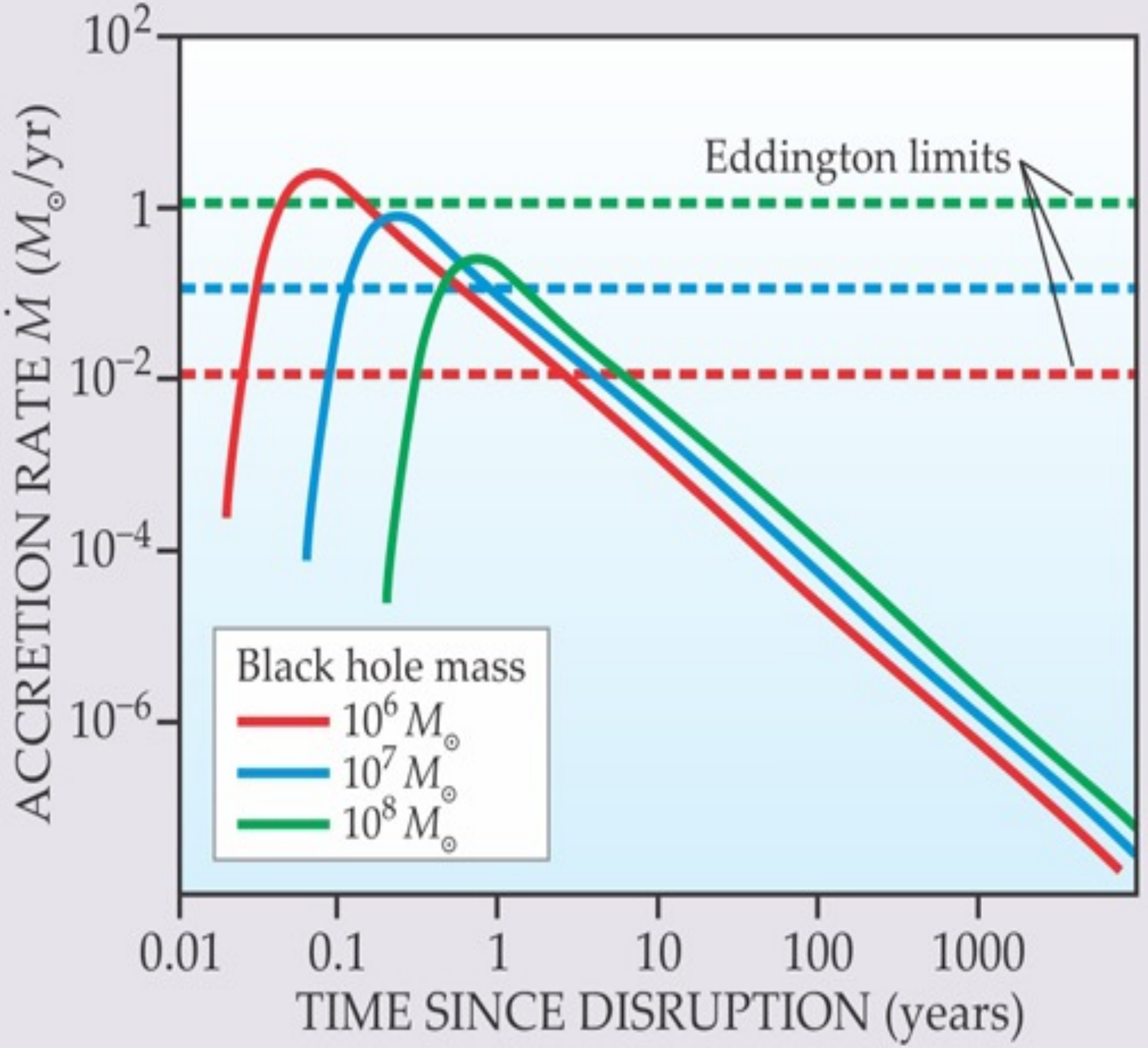

With increasing M_{BH} the rise time to peak accretion increases; the peak accretion rate decreases.

For light black holes, the peak accretion rate exceeds the Eddington limit.

At late time, the accretion rate exhibits fiducial $\propto t^{-5/3}$ (but not always).

(De Colle et al. 2012)

$$t_{\rm dyn} \simeq 14\,{\rm hours} \left(\frac{M_{\rm BH}}{10^7\,M_\odot}\right) \left(\frac{r}{100\,r_{\rm g}}\right)^{3/2} \tag{2}$$

The thermal timescale is the typical timescale for the disk cooling or heating, and thus further depends on the viscosity parameter:

$$t_{\rm th} = t_{\rm dyn}/\alpha \simeq 19\,{\rm days} \left(\frac{M_{\rm BH}}{10^7\,M_\odot}\right) \left(\frac{r}{100\,r_{\rm g}}\right)^{3/2} \left(\frac{\alpha}{0.03}\right)^{-1}. \tag{3}$$

Cooling or heating fronts may travel throughout the disk on longer timescales, accounting for the disk geometry:

$$t_{\rm front} = t_{\rm th}/(h/r) \simeq 380\,{\rm days} \left(\frac{M_{\rm BH}}{10^7\,M_\odot}\right) \left(\frac{r}{100\,r_{\rm g}}\right)^{3/2} \left(\frac{\alpha}{0.03}\right)^{-1} \left(\frac{h/r}{0.05}\right)^{-1}. \tag{4}$$

Finally, the viscous timescale, over which material travels radially from a radius r to the BH, is yet longer:

$$t_\nu = t_{\rm front}/(h/r) \simeq 21\,{\rm years} \left(\frac{M_{\rm BH}}{10^7\,M_\odot}\right) \left(\frac{r}{100\,r_{\rm g}}\right)^{3/2} \left(\frac{\alpha}{0.03}\right)^{-1} \left(\frac{h/r}{0.05}\right)^{-2}. \tag{5}$$

(Trakhtenbrot et al. 2019; W. Zhang et al. 2015)

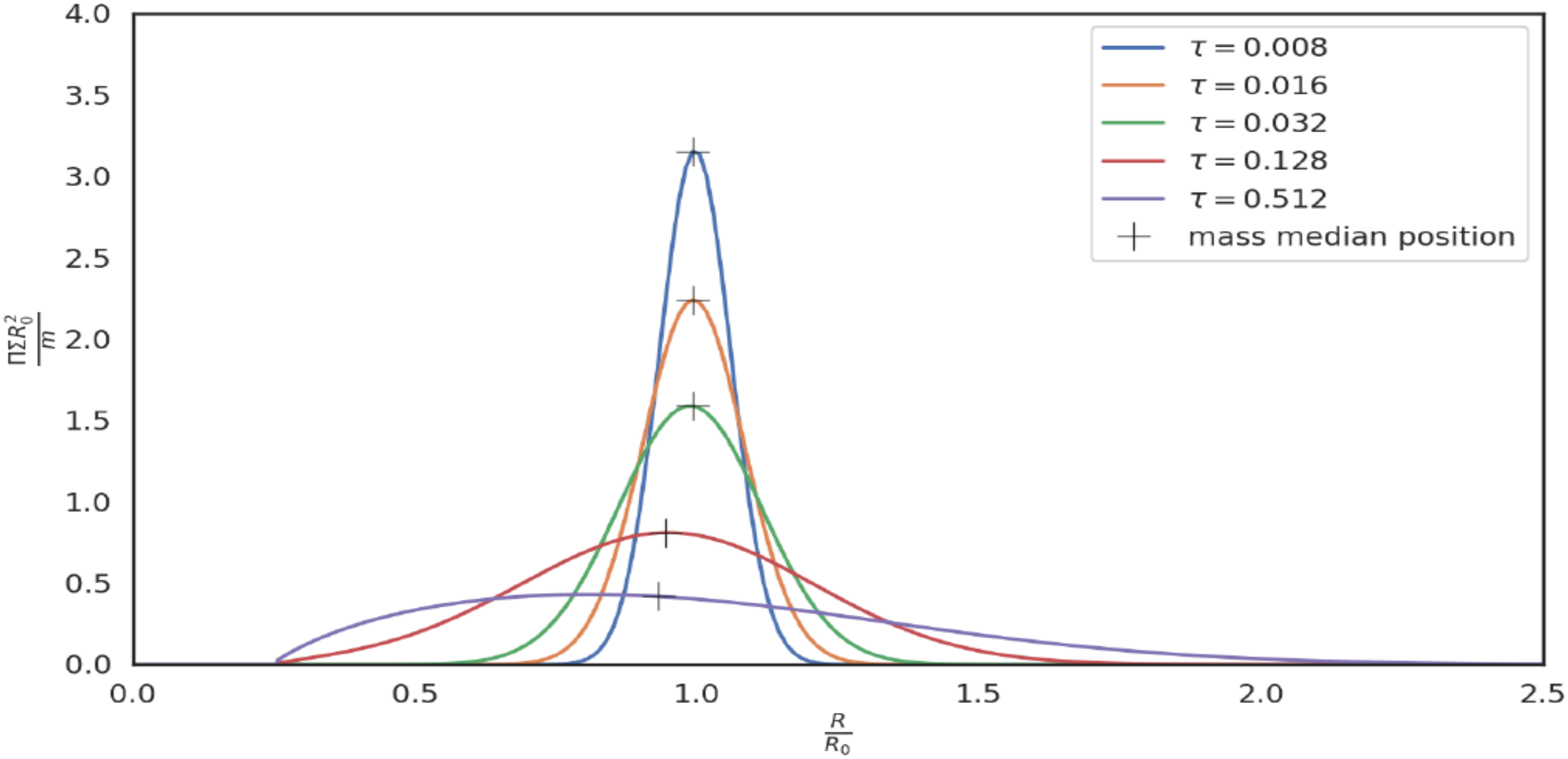

Figure 2.7: Numerical solution to the diffusion equation (1.40) describing the evolution of the surface density profile of the initial mass ring located at $R_0 = 23.6R_g$ with boundary conditions $\Sigma(R_{inner} = 6R_g, t) = \Sigma(R_{outer}, t) = 0$. Black crosses mark the margin for the half of mass of the accretion disc at a given time.

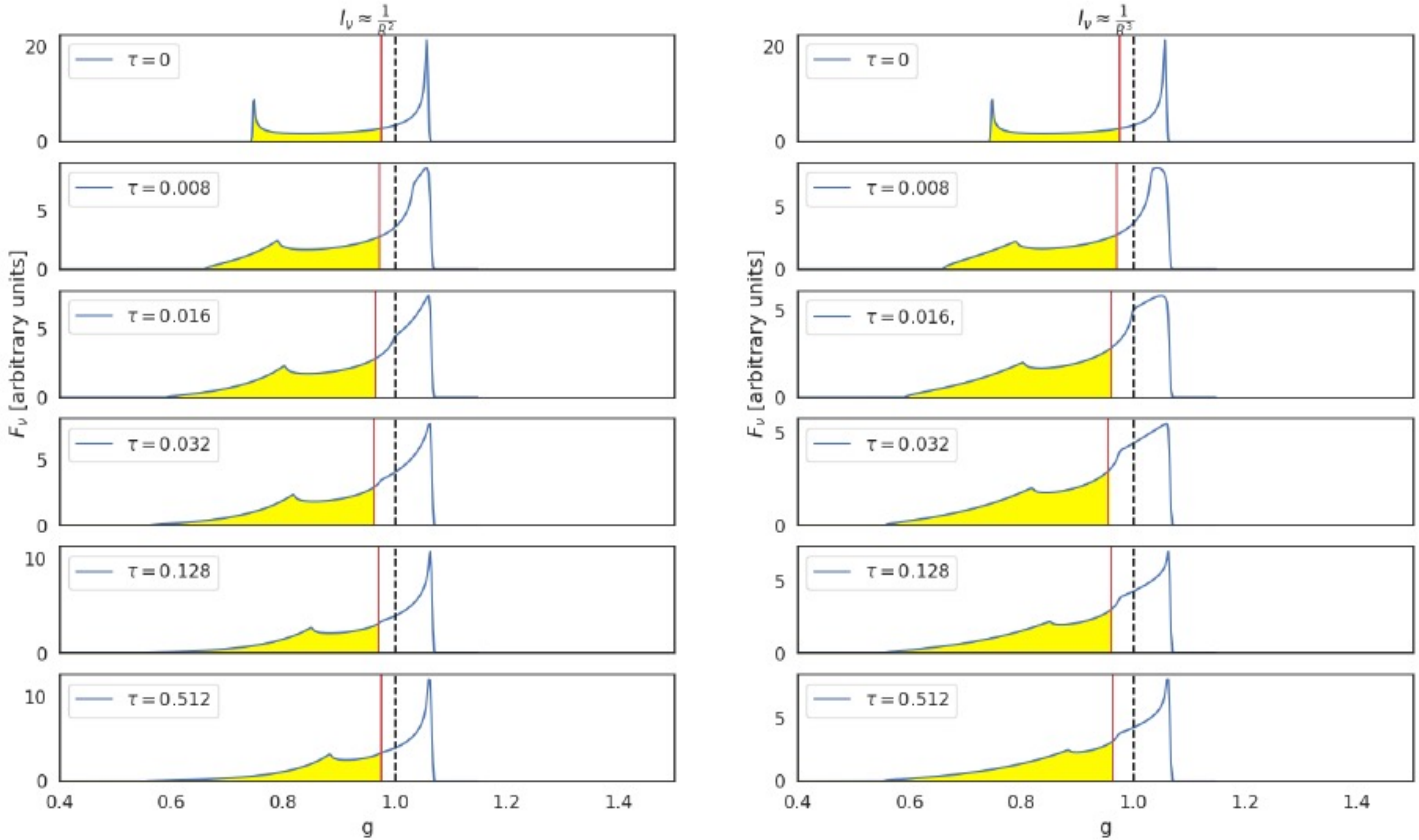

(M. Štolc 2019)

Figure 2.14: Spectral line profile evolution for the system set-up D with the inclination $I = 35$ deg, with the initial radiation intensity $I_\nu \approx \frac{1}{R^2}$ (left panel) and $I_\nu \approx \frac{1}{R^3}$ (right panel). Black dotted line marks the intrinsic frequency, red line marks the centroid energy of a given spectral line.

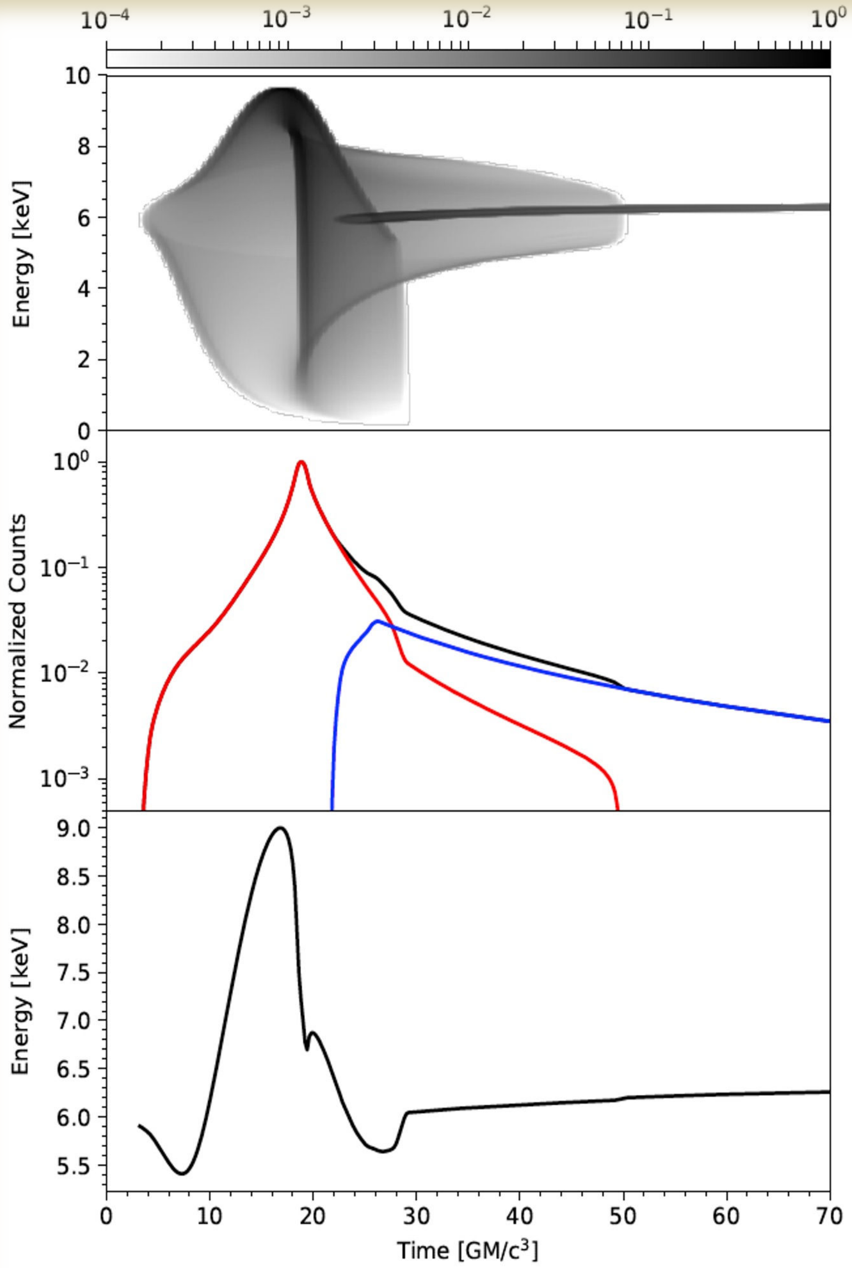

Figure 1. Top panel: the evolution of the fluorescent iron line emission originated from a BP disc. Parameters: black hole spin $a = 0.9987$, inner disc inclination: $i_{\rm in} = 85°$, outer disc inclination: 5°, and truncation radius $r_{\rm BP} = 20$ GM/c^2. Middle panel: lightcurve of the iron line emission. The contribution from inner and outer discs are plotted in red and blue solid lines, respectively; while the black solid line represents the sum of the two. Bottom panel: time evolution of centroid iron line energy. For definition of the centroid line energy one is referred to Paper I.

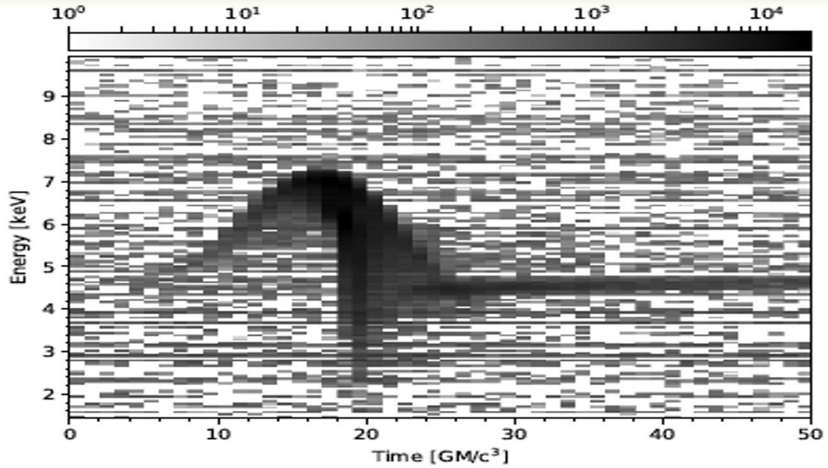

Figure 8. The residuals of the simulated *eXTP*/LAD spectra with respect to a power-law continuum, for Swift J1644+57 (z=0.354). The parameters are: $a = 0.9987$, $i_{\rm in} = 85°$, $i_{\rm out} = 5°$, and $r_{\rm BP} = 20$ GM/c^2. Here we take the black hole mass to be 10^8 M$_\odot$, and the time resolution to be 1 GM/c^3. In the spectrum both the "loop" contributed by the inner disc and the "tail" by the outer disc are seen.

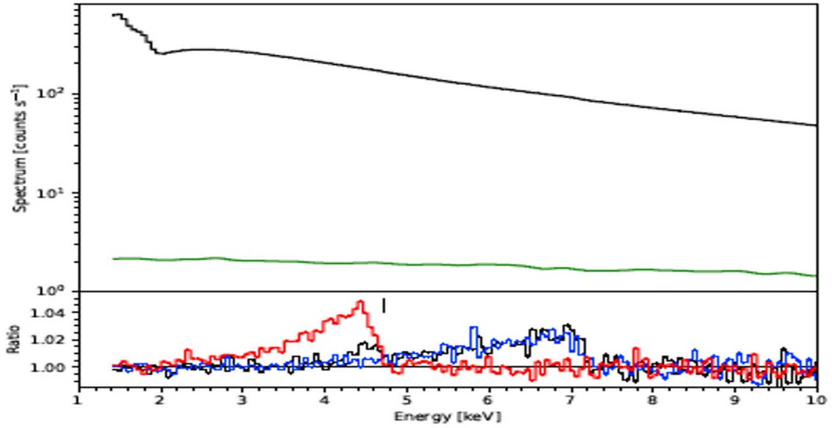

Figure 9. The background-subtracted, time-averaged spectrum (the upper panel) and the data-to-continuum ratio (the lower panel) corresponding to Fig. 8. The background level is plotted in green colour. In the bottom panel the observer frame line energy is indicated by a vertical line. We also plot the data-to-continuum ratio for aligned discs that extend down to ISCO, with inclinations of 5° (red) and 85° (blue), respectively in the lower panel.

(W. Zhang *et al.* 2019)

THANK YOU!